Measurement depth of the cosmic ray soil moisture probe affected by hydrogen from various sources

Trenton E. Franz,[1] M. Zreda,[1] T. P. A. Ferre,[1] R. Rosolem,[1] C. Zweck,[1] S. Stillman,[2] X. Zeng,[2] and W. J. Shuttleworth[1,2]

Received 13 January 2012; revised 8 May 2012; accepted 4 July 2012; published 21 August 2012.

[1] We present here a simple and robust framework for quantifying the effective sensor depth of cosmic ray soil moisture neutron probes such that reliable water fluxes may be computed from a time series of cosmic ray soil moisture. In particular, we describe how the neutron signal depends on three near-surface hydrogen sources: surface water, soil moisture, and lattice water (water in minerals present in soil solids) and also their vertical variations. Through a combined modeling study of one-dimensional water flow in soil and neutron transport in the atmosphere and subsurface, we compare average water content between the simulated soil moisture profiles and the universal calibration equation which is used to estimate water content from neutron counts. By using a linear sensitivity weighting function, we find that during evaporation and drainage periods the RMSE of the two average water contents is 0.0070 $m^3\ m^{-3}$ with a maximum deviation of 0.010 $m^3\ m^{-3}$ for a range of soil types. During infiltration, the RMSE is 0.011 $m^3\ m^{-3}$ with a maximum deviation of 0.020 $m^3\ m^{-3}$, where piston like flow conditions exists for the homogeneous isotropic media. Because piston flow is unlikely during natural conditions at the horizontal scale of hundreds of meters that is measured by the cosmic ray probe, this modeled deviation of 0.020 $m^3\ m^{-3}$ represents the worst case scenario for cosmic ray sensing of soil moisture. Comparison of cosmic ray soil moisture data and a distributed sensor soil moisture network in Southern Arizona indicates an RMSE of 0.011 $m^3\ m^{-3}$ over a 6 month study period.

Citation: Franz, T. E., M. Zreda, T. P. A. Ferre, R. Rosolem, C. Zweck, S. Stillman, X. Zeng, and W. J. Shuttleworth (2012), Measurement depth of the cosmic ray soil moisture probe affected by hydrogen from various sources, *Water Resour. Res.*, *48*, W08515, doi:10.1029/2012WR011871.

1. Introduction

[2] While advances in airborne and space based remote sensing have made significant steps forward in the area of soil moisture [*Robinson et al.*, 2008], there are still significant deficiencies at many spatial and temporal scales. Additionally, the use of indirect methods creates new challenging problems given the dependence of the support volume on the observed quantity [*Binley and Beven*, 2003; *Day-Lewis and Lane*, 2004]. This dependence increases measurement uncertainty and complicates the estimates of fluxes and parameters that control them. The problem is widely recognized and advances in geophysical models have made significant progress in understanding the support volume in several techniques including: time domain reflectometry (TDR) [*Ferre et al.*, 1996], ground penetrating radar [*Day-Lewis et al.*, 2005], electromagnetic induction [*Callegary et al.*, 2007; *McNeill*, 1980], and direct current resistivity [*Furman et al.*, 2003].

[3] In the current research, we are investigating the new technology of cosmic ray neutron probes (Hydroinnova LLC, Albuquerque, New Mexico, USA) for quantifying soil moisture at the landscape scale [*Zreda et al.*, 2008], which is implemented in the cosmic ray soil moisture observing system (COSMOS), a new national network designed for improving hydrometeorological forecasting [*Zreda et al.*, 2012] (data available at http://cosmos.hwr.arizona.edu/). By using a Monte Carlo particle transport code [*Pelowitz*, 2005], the probe has been found to have an effective horizontal footprint of 335 m in radius at sea level with a weak dependence on soil moisture [*Zreda et al.*, 2008]. However, the probe effective depth has a strong dependence on soil moisture and varies from 70 cm in dry soils to 12 cm at full saturation for uniformly distributed soil moisture [*Zreda et al.*, 2008]. As an additional complication, and potentially exciting scientific advance, the probe senses all hydrogen present in the support volume, including water in vegetation, water or snow on vegetation (intercepted precipitation), water or snow on the ground surface [*Desilets et al.*, 2010], water vapor [*Rosolem et al.*, 2011], and water in the minerals present in soils.

[1]Department of Hydrology and Water Resources, University of Arizona, Tucson, Arizona, USA.
[2]Department of Atmospheric Sciences, University of Arizona, Tucson, Arizona, USA.

Corresponding author: T. E. Franz, Department of Hydrology and Water Resources, University of Arizona, 1133 E. James E Rogers Way, Room 122, Tucson, AZ 85721, USA. (tfranz@email.arizona.edu)

0043-1397/12/2012WR011871

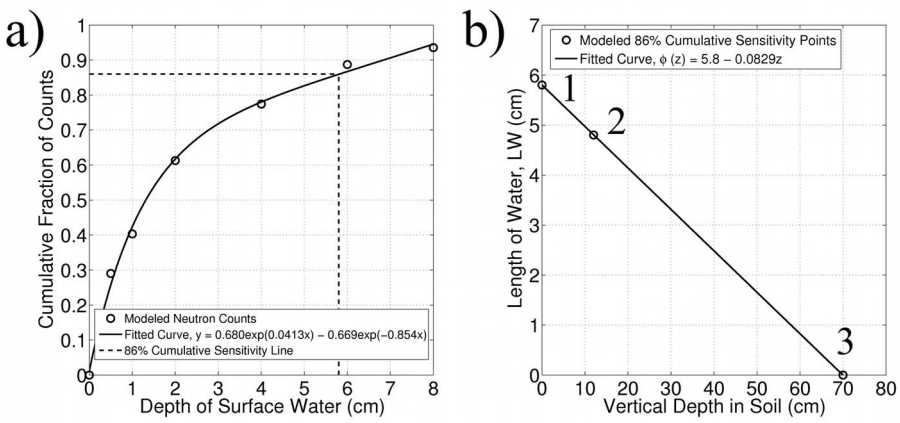

Figure 1. (a) Cumulative fraction of fast neutron counts modeled above the surface as a function of ponded water on the surface (maximum count rate taken at 4 m of water). The 86% cumulative sensitivity point was found to be 5.8 cm for liquid water (this is point 1 in part b). (b) Relationship for the 86% cumulative sensitivity contour in uniform sand derived from three sensitivity points (equation (1)). Points 2 and 3 were computed from the modeled wet and dry cases reported in *Zreda et al.* [2008].

[4] In this work, we develop a framework for estimating the effective measurement depth in soils by accounting for three pools of hydrogen, including water on the ground surface, in the mineral structure of soils, and in the pore space between mineral grains. We then present several cases of varying water content in both the mineral and pore spaces and the corresponding effective measurement depth. We compute the hypothetical distributions of soil water using one-dimensional Richards Equation, use the profiles in a neutron transport model, and compare the modeled average soil moisture between the methods using two different depth-weighting functions. Last, we compare average soil moisture between a cosmic ray neutron probe and a distributed sensor network in Southern Arizona.

2. Methodology

2.1. Development of Effective Sensor Depth Framework

[5] The influence of soil moisture on the intensity of cosmic ray fast neutrons above the surface has been known for several decades [*Hendrick and Edge*, 1966]. The removal of neutrons is dominated by neutron collisions with hydrogen atoms due to the nuclear cross section properties of hydrogen [*Zreda et al.*, 2008]. More recently, fast neutron intensity has been shown to be sensitive to hydrogen present in liquid and frozen water on the ground surface and on the vegetation canopy [*Desilets et al.*, 2010]. However, the sensitivity to multiple hydrogen sources requires accounting of the various sources in order to isolate the source of interest, for example pore water.

[6] The following pools of hydrogen exist at and near the land surface: water vapor in air, liquid and solid water on the surface, liquid and solid water on the vegetation canopy, water vapor in soil, liquid and solid water in soils, water within the minerals in soils (also known as lattice water), and carbohydrates in plant tissue and organic soil horizons. Fortunately, hydrogen in biomass and organic matter in soil is usually small compared to the hydrogen in soil pore space and lattice water contained in the mineral grains. For example, a temperate forest in the northeastern USA has a density of 4 kg m^{-2} (40 tonnes wet biomass per hectare; [*Milbrandt*, 2005]), which is equivalent to approximately 2 mm of water ponded on the surface assuming a reasonable vegetation water content of 50%. For comparison, soil water (pore and lattice) sensed by cosmic ray probes is between 15 mm for dry soils (0.020 m^3 m^{-3}) and 50 mm for saturated soils (0.40 m^3 m^{-3}) [*Zreda et al.*, 2008]. If the amount of hydrogen stored in biomass is not negligible, its effect on the ability to measure soil moisture usually is small because we measure relative changes in neutron counts, and background hydrogen from vegetation, if constant in time, is implicitly included when the sensor is calibrated locally [*Desilets et al.*, 2010]. We note that neutron counts have been shown to be affected by fast growing vegetation, like corn [*Hornbuckle et al.*, 2011], and may require a correction factor for stable soil moisture measurements in time."

[7] Here we consider only hydrogen sources from liquid and solid water on the surface, liquid water in the pore space, and lattice water in the mineral structure, and we assume that the influences of hydrogen in biomass, in organic soils, and organic matter in soils are relatively small or static in time as described above. In previous work, *Zreda et al.* [2008] presented two cases of uniformly distributed dry and fully saturated porous media (uniform quartz sand (100% SiO_2), particle density = 2.65 g cm^{-3}, porosity n = 0.40 m^3 m^{-3}), where the two e-folding depths were quantified with the Monte Carlo Neutron Particle transport code (MCNPx) [*Pelowitz*, 2005]. This two e-folding sample volume can be defined as the volume within which 86% of the detected neutrons above the surface originate. We therefore define this point as the 86% cumulative sensitivity point and the effective depth of the sensor. *Zreda et al.* [2008] found this point varied for uniform wet and dry cases, with depths of 12 and 70 cm, respectively. In a similar fashion, we simulated various depths of liquid water (from 5 mm to 4 m) on dry uniform sand and find 86% of the counted neutron cumulative sensitivity to occur at 5.8 cm of water (Figure 1a).

[8] Using these three 86% cumulative sensitivity points, we construct an 86% cumulative sensitivity contour defined by φ (Figure 1b). For convenience and in order to define a common unit between the different hydrogen sources, we compute the length of water, LW (cm), for each case. For

liquid water, LW is simply the depth of water. For the pore water cases, LW is the pore water content ($m^3\ m^{-3}$) multiplied by the effective depth (cm). For the wet case, LW = 0.4 $m^3\ m^{-3}$ * 12 cm = 4.8 cm, and for the dry case, LW = 0.0 $m^3\ m^{-3}$ * 70 cm = 0 cm. From linear regression of the three sensitivity points ($R^2 > 0.99$, Figure 1b), we define the 86% cumulative sensitivity contour, φ (cm), as,

$$\varphi(z) = 5.8 - 0.0829z \quad 0 \le z \le 70, \tag{1}$$

where z (cm) is the vertical distance in soil, positive downward. The liquid water 86% cumulative sensitivity point determines the intercept in equation (1) and the slope is controlled by the nuclear cross section of the soil (here, SiO_2).

[9] With the 86% cumulative sensitivity contour now defined from the three simple cases, we can generalize the framework to include hydrogen from other sources and with variable vertical distributions. We assume that all hydrogen atoms at the same vertical location affect the neutron intensity with the same efficiency, regardless of their association, and again combine the various pools of hydrogen into the equivalent unit of length of water,

$$LW = W_s + W_L + W_P, \tag{2}$$

where W_S is surface water (cm), W_L is lattice water (cm), and W_P is pore water (cm). We can rewrite equation (2) in units measured in the field and let the function be dependent on soil depth,

$$LW(z) = W_s + \frac{\rho_{bd}(z)\tau(z)z}{\rho_w} + \theta(z)z, \tag{3}$$

where ρ_{bd} is the dry bulk density of soil (g cm^{-3}), ρ_w is the density of liquid water (assumed to be 1 g cm^{-3}), τ is the weight fraction of lattice water in the mineral grains and bound water, defined as the amount of water released at 1000°C preceded by drying at 105°C (g of water per g of dry minerals, herein known as lattice water), and θ is the volumetric pore water ($m^3\ m^{-3}$). By setting the 86% cumulative sensitive contour equal to the sum of all water in the soil profile and on the surface we can define a relationship to derive the effective depth of the sensor, z^* (cm),

$$\varphi(z^*) = W_s + \int_0^{z^*} (\rho_{bd}(z)\tau(z) + \theta(z))dz. \tag{4}$$

For the simple case of no surface water and uniform ρ_{bd}, τ, and θ with depth, we can solve equation (4) for z^*,

$$z^* = \frac{5.8}{\rho_{bd}\tau + \theta + 0.0829}. \tag{5}$$

Neglecting lattice water, z^* ranges between 70 cm for a pore water content of 0 $m^3\ m^{-3}$, and 12 cm for pore water content of 0.40 $m^3\ m^{-3}$, as to be consistent with previous results [*Zreda et al.*, 2008].

2.2. Modeling the Vertical Distribution of Pore Water

[10] To generate different cases of the vertical distribution of pore water we used a numerical solution of the one-dimensional Richards Equation as implemented in the HYDRUS 1-D software [*Simunek et al.*, 2008]. We selected four different soil texture categories to investigate, sand, sandy loam, silt and silty clay loam using the standard ROSETTA parameters [*Schaap et al.*, 2001] for the van Genuchten Mualem hydraulic model with no hysteresis [*Simunek et al.*, 2008]. We set the domain to be a 2 m vertical column with a resolution of 2 cm. The lower boundary condition was set to free drainage. The top boundary condition was set to an atmospheric boundary and varied between a uniform intensity rain-event (two cases: 2.54 cm (1 inch) in 24 h and 7.62 cm (3 inches) in 24 h) followed by a 2 mm d^{-1} potential evapotranspiration boundary condition. The initial conditions for each texture were set to a uniform pressure head of −300 cm to represent field capacity. Each simulation was carried out for a 10 day period.

2.3. Modeling of Neutrons and Conversion to Water Content

[11] To simulate the transport of cosmic ray particles and creation of nucleonic cascades throughout the atmosphere and near the surface we used the fully three-dimensional MCNPx model [*Pelowitz*, 2005]. MCNPx is a general purpose Monte Carlo code that tracks the individual life history of a particle and subsequent particles as it interacts with other materials in the domain through its nuclear cross section. For the simulations, we use a similar setup as those reported in *Zreda et al.* [2008] but with vertical variations in the distribution of pore water. At 8 km above the surface, a distribution of high-energy neutrons are projected toward the earth, where the atmosphere is represented by vertical layers of dry air in a 2 × 2 km domain with periodic boundary conditions. At 1 to 2 m above the surface we record the fast neutron flux, which corresponds to the same energy level as the cosmic ray neutron detector, which counts individual neutrons. We assume the relative sensitivity of modeled fast neutron flux and observed counted neutrons is equivalent. We include only vertical heterogeneity in the soil water layers as fully three-dimensional variations in pore water in MCNPx are beyond the scope of this work and remain a challenging research problem. In regards to including only vertical pore water variability, we note that neutrons mix rapidly above the surface (fast neutron velocities >10 km s^{-1} [*Glasstone and Edlund*, 1952]) and form a well-mixed layer of neutrons representative of the entire footprint. From multiple calibration data sets, at a single site, over a range of water contents and horizontal heterogeneity [*Zreda et al.*, 2008; *Zreda et al.*, 2012], we find that horizontal heterogeneity likely plays a minor role but the issue remains to be fully validated. By using only vertical layers we are able to use the one-dimensional HYDRUS modeling results directly. For the simulations, we use a material input of pure quartz (SiO_2) for the soil water layers. For each case, a number of particles are simulated (typically 1,000,000) making sure the 10 statistical model tests are satisfied when calculating the fast neutron flux at the 1 to 2 m layer [*Pelowitz*, 2005]. Finally, we use the universal calibration equation [*Desilets et al.*, 2010] to convert relative neutron counts/flux into soil moisture,

$$\theta(N) = \frac{0.0808}{\left(\frac{N}{N_0}\right) - 0.372} - 0.115, \tag{6}$$

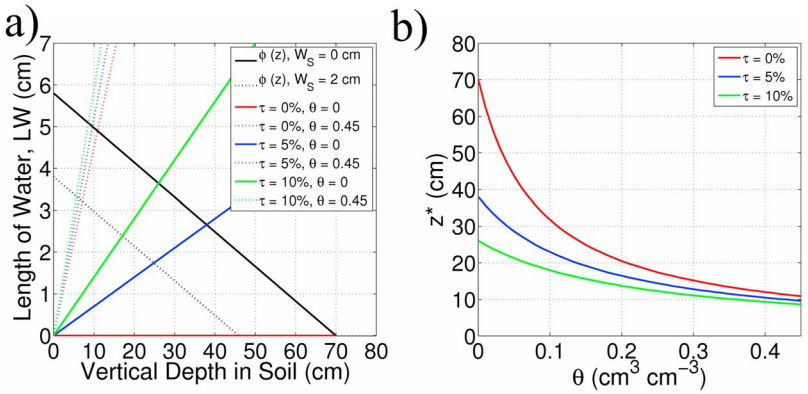

Figure 2. (a) Length of water as a function of soil depth for different lattice water and uniform dry or wet soil moisture profiles. The effective sensor depth, z^*, for each case is where the sum of water crosses the 86% cumulative sensitivity contour, φ. (b) Relationship of effective sensor depth, z* (equation (5)), for all uniform soil moisture profiles, three cases of lattice water, and no ponded water on surface calculated with equation (4). Note ρ_{bd} = 1.4 g cm^{-3} for all cases, τ is the weight fraction of lattice water in mineral grains, θ is the volumetric pore water, and W_S is the surface water.

where N is the neutron counting rate/flux normalized to a reference atmospheric pressure and solar activity level and N_0 is the counting rate/flux over dry soil under the same reference conditions.

3. Results

3.1. Uniform Profiles of Hydrogen

[12] First, we investigate how the effective sensor depth varies with uniform vertical profiles of different lattice water and pore water. For these conditions, the length of water increases linearly with depth. Figure 2a illustrates three cases of different lattice water and pore water conditions. The effective sensor depth, z^*, is defined as the depth at which the sum of surface, pore, and lattice water crosses the 86% cumulative sensitivity contour (section 2.1, equation (4)). In Figure 2a we also illustrate how the relative position of the 86% cumulative sensitivity contour would vary for no ponded water and 2 cm of ponded water on the surface. The values of z^*, computed using equation (5) for different water contents and three different lattice water values (Figure 2b) show the nonlinear reduction in z^* for increasing lattice water. The large reductions in z^* with changes in water content under dry conditions are expected because of the relatively high sensitivity of the neutron probe's response under dry conditions. The value of z^* is relatively independent of lattice water content at high water contents.

[13] Hydrogen in lattice water contributes to the reduction of z* values (Figure 2). But lattice water is rarely reported in the literature and we know little about its variations in soils. Despite the recognition of lattice water in soils and its potential influence on neutron counts [*Gardner and Kirkham*, 1952], it was mostly ignored given the locality of the in situ neutron probes and site specific calibration procedures [*Chanasyk and Naeth*, 1996; *Evett and Steiner*, 1995]. Because lattice water can significantly affect neutron counts, we measure lattice water in soils at COSMOS sites as part of the standard calibration procedure. The analysis is performed using gravimetric methods in a laboratory (we use Actlabs, Ancaster, Ontario, Canada) on various samples collected within the probe footprint. We found significantly higher lattice water in the volcanic soils of Hawaii (average of 12.6 $\pm$ 7.26% by weight for three sites) compared to those from the continental USA (average of 3.64 $\pm$ 1.55% for 41 sites, full data available at http://cosmos.hwr.arizona.edu/). Previous research [*Greacen*, 1981] showed a linear relationship between lattice water and clay content. But our results suggest a more complex relationship. Lattice water is present not only in clay minerals, but also in many common rock-forming primary minerals such as hornblende and biotite and requires further research.

3.2. Variable Profiles of Pore Water

[14] In addition to the uniform case (section 3.1), we investigate how vertical variations in soil moisture affect the effective measurement depth. Using a one-dimensional modeling experiment, we simulate the temporal distribution of soil moisture in various homogeneous porous media for two prescribed atmospheric boundary conditions. Figures 3a and 3c show the infiltration, redistribution, and evaporation of water in uniform sand and silty clay loam for a 7.62 rain event over 24 h followed by a 2 mm d^{-1} potential evapotranspiration. Note, the boundary conditions were chosen to avoid surface runoff and that the simulations showed similar behavior for the 2.54 cm rain event for each soil texture and where not shown. There are large differences in the wetting front and total infiltration of water for the two different textures. As soil moisture is redistributed in time, the effective measurement depths change (Figures 3b and 3d). Specifically, the effective depth becomes shallower when surface layers are wetter, and deeper with drier surface layers. There is a significant difference between the two cases: given the differences in field capacity (and thus also the initial water content) between the two soils, we see a reduced range in z^* values of 9 to 15 cm for the silty clay loam (Figure 3d) as compared to 15 to 45 cm for the sand (Figure 3b), for the same precipitation and evaporation boundary conditions.

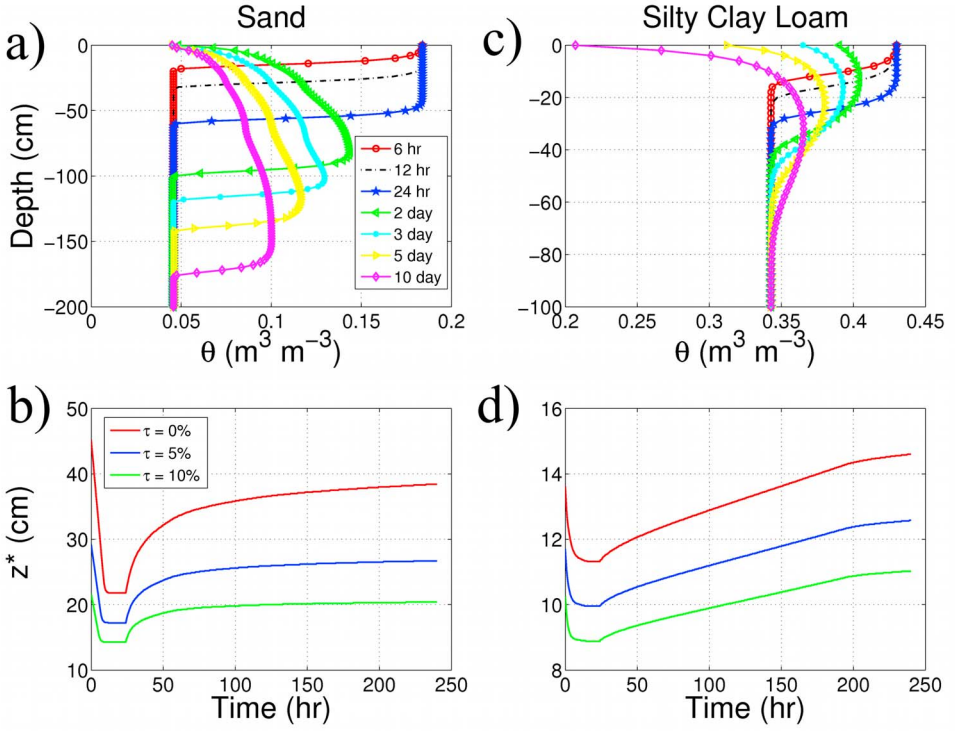

Figure 3. Soil moisture profiles generated from a solution of one-dimensional Richards Equation for a uniform (a) sand and (c) silty clay loam using a top boundary condition of 7.62 cm of rain in 24 h followed by a switch to 2 mm d^{-1} potential evapotranspiration using the van-Genuchten mualem hydraulic model (ROSETTA) [*Schaap et al.* 2001]. (b and d) Corresponding time series of z^* values (equation (4)) with various lattice water values. Note ρ_{bd} = 1.4 g cm^{-3} for all cases and no runoff was generated from these boundary conditions.

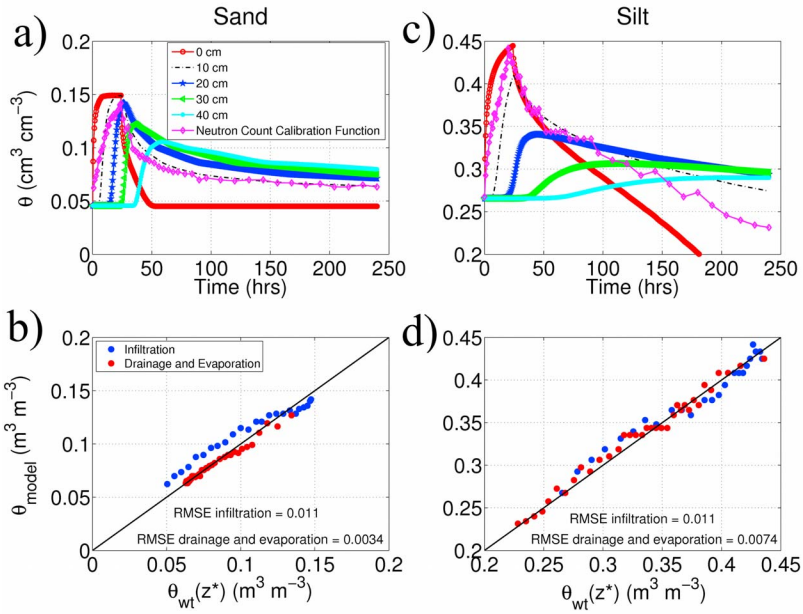

Figure 4. (a and c) Depth specific time series of soil moisture and corresponding average soil moisture computed with neutron modeling and converted into soil moisture using the universal calibration function (equation (6)) for a 2.54 cm rain event over 24 h followed by a 2 mm d^{-1} PET top boundary, for uniform (a) sand and for (c) silt. (b and d) Corresponding average water contents from neutron calibration model (y axis) and profiles using linear weighted average with a known z* (equations (4) and (7)) from the HYDRUS soil moisture profiles (x axis).

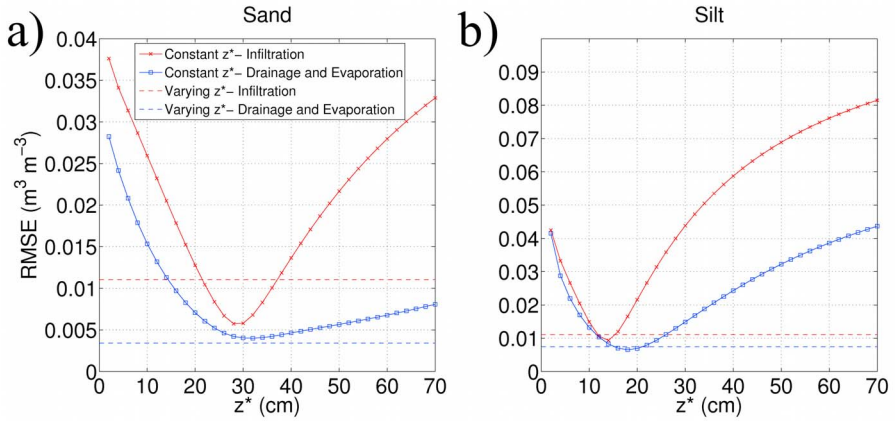

Figure 5. RMSE of average water content computed with neutron simulations (equation (6)) versus linear depth weighting of the HYDRUS soil moisture profiles (equation (7)) for constant and varying z* values (equation (4)) for (a) sand and (b) silt cases presented in Figure 4. Varying z^* weighting performs better or the same for both cases during drainage and evaporation soil moisture stage, which will usually dominate annual time series.

3.3. Comparison of Modeled Average Soil Moisture

[15] Using the simulated changes of water content with time from the HYDRUS model, we computed, using MCNPx, the equivalent neutron counts that a cosmic ray sensor would observe. With the modeled neutron counts and using equation (6) [*Desilets et al.*, 2010], we compared the average modeled soil moisture to the simulated HYDRUS depth weighted values (Figure 4) in order to test the validity of the proposed framework. We used the HYDRUS depth profiles to calculate a z^* value (equation (4)) and then report the weighted average of soil moisture using only those layers above z^*. In addition to a uniform weight profile (each layer is assigned the same weight), we calculated a weighted depth profile, *wt*, according to:

$$wt(z) = a\left(1 - \left(\frac{z}{z^*}\right)^b\right) \quad 0 \le wt \le z^*, \tag{7}$$

where a is a constant defined by the condition that the weights are conserved, $1 = \int_0^{z^*} a\left(1 - (z/z^*)^b\right)dz$, which yields the solution $a = 1/(z^* - \{z^{*b+1}/[z^{*b}(b+1)]\})$, and b controls the curvature of the weighting function where we assumed a value of 1 for a linear relationship. The value of b and other higher-order depth weighting functions are discussed elsewhere with numerical sensitivity analyses using a neutron transport model [*Zweck et al.*, 2011] and theoretical calculations of neutron cross sections (Desilets et al. 2012, unpublished).

[16] We compare the neutron modeled average soil moisture (equation (6)) to the depth weighted average value for two different soil types and using two different depth-weighting schemes (uniform and linear). With the linear depth weighting, we find the RMSE of soil moisture during infiltration for both soil types is 0.011 $m^3\ m^{-3}$ with a maximum deviation of approximately 0.020 $m^3\ m^{-3}$ (Figures 4b and 4d). With the uniform depth weighting, the RMSE is 0.025 $m^3\ m^{-3}$ with a maximum deviation of approximately 0.050 $m^3\ m^{-3}$. During drainage and evaporation, the RMSE for both soil types is less than 0.0070 $m^3\ m^{-3}$ with a maximum deviation of approximately 0.010 $m^3\ m^{-3}$ for the linear weighting and an RMSE of 0.0090 $m^3\ m^{-3}$ and maximum deviation of 0.020 $m^3\ m^{-3}$ for uniform weighting.

[17] As an additional experiment on the validity and uncertainty of the depth weighting function, we compute the RMSE during infiltration and drainage and evaporation for constant and varying z^* values (Figure 5). We find during drainage and evaporation the varying z^* value performs better or the same as all ranges of z^* values. During infiltration we find the varying z^* performs slightly worse than the optimal constant z^* for sand and about the same for silt. The analysis suggests that guesses within a few centimeters of the true z^* do not greatly increase the overall RMSE. Given some prior information about the system (like soil texture class or one known calibration point) reasonable first guesses of z^* can likely be made from neutron count data alone, as implemented on the COSMOS website (see http://cosmos.hwr.arizona.edu/). We note that sharp wetting fronts that exist during the sand case are worst case scenarios and that infiltration periods are usually short compared to drainage and evaporation periods for typical soil moisture time series. Section 4.1 will discuss this issue in greater detail.

[18] As would be expected, all four modeled soil types show hysteretic behavior of soil moisture deviation due to the relative depth of the wetter part of the profiles during infiltration and drainage (Figure 6). The hysteretic effects are greatest for the coarse textured soils of sand and sandy loam, given the existence of relatively sharp wetting fronts during infiltration. Figure 6 illustrates the potential nonuniqueness in modeled neutron counts versus depth weighted average water content with maximum deviations on the order of 0.020 $m^3\ m^{-3}$. It is important to note that the peak soil moisture for all soils (Figure 4) was preserved in the comparison, presumably because the wetting front passed the minimum or saturated z* value. Section 4.1 will discuss this issue in more detail.

3.4. Comparison of Observed Average Soil Moisture

[19] As a field validation of the linear depth-weighting framework, we compare the estimated soil moisture from a cosmic ray neutron probe and the mean value from a

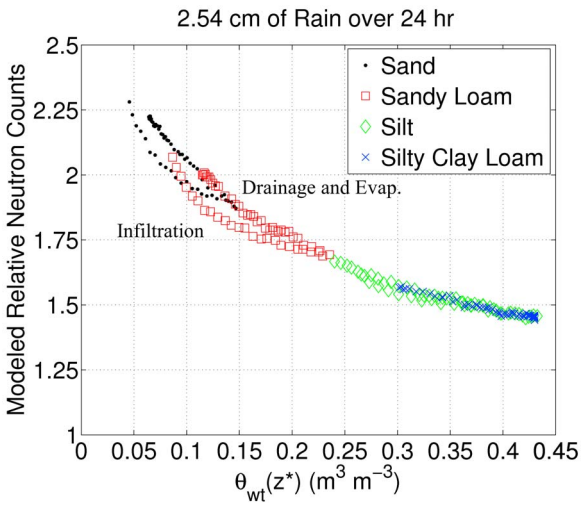

Figure 6. Modeled relative neutron counts (normalized to pure water case) of four soil types versus the linear depth weighted water content value (equations (4) and (7)) for a 2.54 cm rain event. Coarser soils illustrate greater non-uniqueness than finer textured soils because of the sharp wetting fronts that exist during infiltration. Note the size of the hysteretic loop would be approximately double for uniform weighting.

distributed sensor network. The full observational design, measurement uncertainty, spatial heterogeneity, and site description are described elsewhere [*Franz et al.*, 2011; Franz et al., 2012, unpublished]. Here we compare the mean water content time series within the footprint. In June 2011, 180 time domain transmission (TDT) (Model ACC-SEN-TDT from Acclima Inc., Meridian, ID, USA) sensors were installed

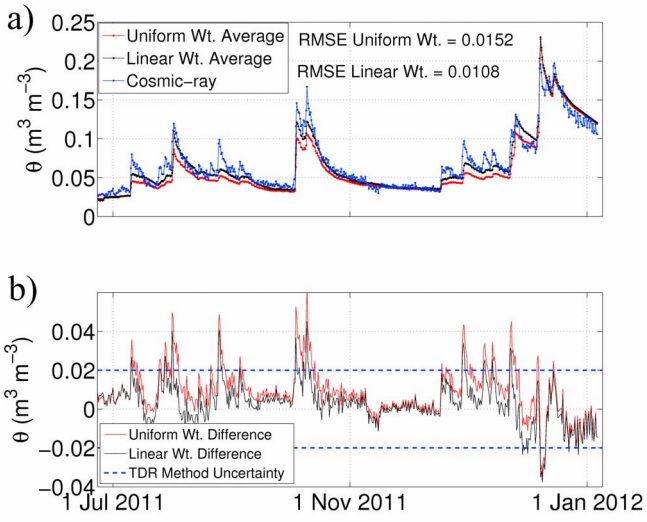

Figure 7. (a) Comparison of areal average soil moisture between a cosmic ray neutron probe (equation (6)) and a distributed sensor network over a 6 month period in southern Arizona. (b) Time series of differences between average soil moisture for uniform and linear depth weighting functions (equations (4) and (7)). Note data are all averaged over a 6 h period and a majority fall within TDR uncertainty bounds.

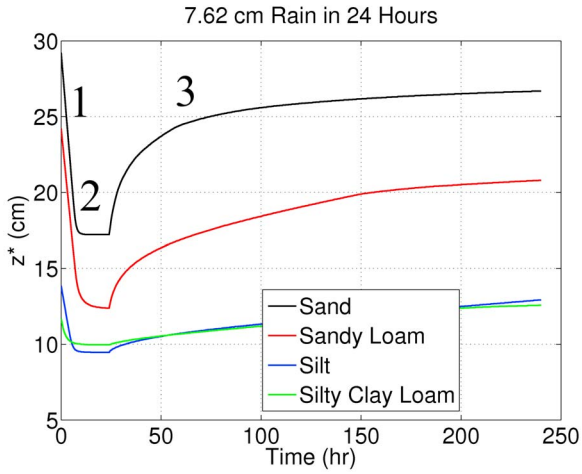

Figure 8. Time series of z^* values (equation (4)) for four soil types and 7.62 cm rain event. All soils display characteristic behavior of z* values during different soil moisture stages: stage 1 infiltration, linear decrease in z^* for piston flow; stage 2 early time drainage and evaporation, flat z^*; stage 3 late time drainage and evaporation, z^* returns to original value following characteristic $t^{1/2}$ behavior.

around a cosmic ray footprint at Santa Rita Experimental Range in Southern Arizona (31.9085°N 110.8394°W). TDT sensors were placed beneath the canopy and in the intercanopy space at 18 locations around the footprint—every 60° and at radii of 25, 75, 200 m—at vertical depths of 10, 20, 30, 50, and 70 cm, and recorded volumetric water content every 30 min. For the experiment each TDT sensor was calibrated both in the laboratory and in the field.

[20] To compare the cosmic ray derived soil moisture with the TDT data, each radial location was given equal weight and then vertically averaged using uniform and linear depth-weighted function described above. The time series of soil moisture for the cosmic ray neutron probe, uniform weighted average of the TDT network, and the linear weighted average indicate good agreement over the 6 month study period (Figure 7a). Differences between the two sensors and weighting schemes are small with an RMSE of 0.015 $m^3\ m^{-3}$ for the uniform weighting and 0.011 for the linear weighting (Figure 7b). The largest deviations of 0.040 $m^3\ m^{-3}$ occur during peak soil moisture periods when sharp wetting fronts are likely present in the sandy loam soils and the dynamics in the top 5 cm may not be adequately captured. We note that a majority of the time series is well within the accepted TDR uncertainty limits [*Topp et al.*, 1980] and that the overall agreement is reasonable in this highly heterogeneous soil moisture environment [*Franz et al.*, 2011].

4. Discussion

4.1. Estimating Effective Sensor Depth

[21] With the simple model of infiltration, redistribution, and evaporation we investigated the changes in z^* for four soil textures (Figure 8). There are three distinct stages in the behavior of z^* values. The first stage is the linear decrease in z^* during piston flow where the sensor has the greatest uncertainty for reasons discussed in section 3.3. Stage 1

transitions into stage 2 when the probe becomes insensitive to additional hydrogen atoms in the support volume and z^* is constant. Stage 3 begins when the probe once again becomes sensitive to changes in hydrogen atoms in the support volume due to drying and vertical redistribution of water out of the support volume. Here we see a gradual increase in z^* back to the initial z^* for dry conditions, which follows the characteristic $t^{1/2}$ shape commonly found in infiltration and drainage equations [*Bear*, 1972; *Philip*, 1969]. While identifying the transition points between the three stages of z^* requires some prior knowledge of the porous medium properties, we are able to connect the stages with the underlying physics governing the system. By identifying these physical processes we are able to better describe the range of expected uncertainty in the measurements that can be used in subsequent analyses. We hypothesize that with further research it may be possible to determine the stage of z^* behavior from time series of neutron data alone.

4.2. Representativeness of Areal Average Soil Moisture Using a Cosmic Ray Neutron Probe

[22] We have presented a simple and robust framework to estimate the effective sensor depth given three sources of hydrogen—surface, lattice, and pore water—and their vertical variations in the soil profile. For four soil types, we found that the cosmic ray sensor tends to overestimate soil moisture during infiltration with a RMSE of only 0.011 m^3 m^{-3} for a linear depth-weighting function (Figure 4). In addition to preserving peak soil moisture, the sensor performs well during the drainage and evaporation stage with a RMSE of less than 0.0070 m^3 m^{-3} when using effective sensor depth. Furthermore, most natural sites will have annual time series of soil moisture that are dominated by long decay periods, except for heavily irrigated locations and humid locations with frequent rain events. Comparison of a cosmic ray neutron probe and a distributed sensor soil moisture network in Southern Arizona indicated good agreement with a RMSE of 0.011 m^3 m^{-3} over a 6 month study period.

[23] As a worst case scenario of wet over dry soils with a sharp wetting front, we find the sensor overestimates water content by up to 0.020 m^3 m^{-3}. However, we note that this state of soil moisture is highly unstable given: (1) the high variability of natural rain events [*Katul et al.*, 2007]; (2) variable vertical infiltration processes at a range of spatial scales; (3) the homogenizing effects of flow through porous media [*Hillel*, 1998]; (4) spatial smoothing of soil moisture over large areas [*Grayson et al.*, 1997] (cosmic ray probe footprint ~335 m in radius); and (5) the temporal smoothing due to the long time needed to obtain good neutron counting statistics (at least 1 h to obtain 0.020 m^3 m^{-3} water content error in cosmic ray sensors) [*Zreda et al.*, 2008]. In addition, ancillary information such as rainfall can help identify potential periods of overshoots in cosmic ray sensor data. Those data points can then be flagged and a larger range of uncertainty can be associated with them in subsequent analyses such as data assimilation or coupled hydrogeophysical inversion [*Hinnell et al.*, 2010].

4.3. Limitations of This Study

[24] In this research, we presented a framework to understand the effective cosmic ray sensor depth given three pools of hydrogen on the surface and within a few decimeters of the soil profile. Clearly there are additional sources of hydrogen that may need to be accounted for in other situations, especially if they are changing significantly over time. At the time of calibration, background hydrogen sources will be accounted for in the N_0 parameter in equation (6). However, fast growing crops such as corn have been shown to affect the N_0 parameter by 10% at full height or 6 mm or liquid water equivalent [*Hornbuckle et al.*, 2011]. Initial analysis of various COSMOS site data reveals a persistent diurnal cycle in fast neutrons on the order 0.010 m^3 m^{-3} soil water content. It is unclear whether the diurnal cycles are due to electronic sensitivity, natural fluctuations of incoming cosmic rays, changes in atmospheric water vapor [*Rosolem et al.*, 2011], or vertical redistribution of water in soils or plants between the night and day. As we begin to quantify COSMOS site-specific z^* values, we are finding certain conditions, such as the presence of deep organic layers and high lattice water, that lead to small effective depths, sometimes approaching the liquid water value of 6 cm. These small depths will display greater and faster soil moisture dynamics compared with the dynamics associated with effective depths of tens of centimeters [*Katul et al.*, 2007] but will be more comparable to passive microwaves [*Jackson et al.*, 1997]. We also note that the presented framework only considers 86% of the neutron sensitivity, with 14% of the sensitivity residing below the estimated z^* value, which may explain some of the remaining uncertainty. Future work will resolve some of these issues with additional field experiments, neutron modeling, and analysis using both the fast and thermal energy neutron counts as thermal neutrons may have different sensitivity to changes in hydrogen from vegetation and snow sources [*Desilets et al.*, 2010].

5. Conclusions

[25] In this work, we found it was possible to create a simple and robust framework for calculating the effective sensor depth of a cosmic ray neutron probe while accounting for three sources of hydrogen and their vertical variability. We found for a suite of plausible soil water profiles that MCNPx modeled average soil moisture compared well with the depth weighted average soil moisture of the same profiles (0.010 m^3 m^{-3} RMSE), indicating the validity of the presented framework. As an additional validation, we found similar agreement between 6 months of observed soil moisture data at a site in Southern Arizona and the hypothetical modeling. With the increased use of cosmic ray sensors over a diverse range of study sites and conditions, we need additional experiments and tools to decouple the various pools of hydrogen that may exist at or near the surface.

[26] **Acknowledgments.** This research and the COSMOS project were supported by the U.S. National Science Foundation grant AGS-0838491. We would like to thank three anonymous reviewers, the associate editor, and John Selker for their helpful reviews. We would also like to thank, COSMOS site collaborators, Darin Desilets of Sandia National Laboratories, Hydroinnova, Gary Womack of Questa Instruments, and Santa Rita Experimental Range for their support.

References

Bear, J. (1972), *Dynamics of Fluids in Porous Media*, Elsevier, New York.

Binley, A., and K. Beven (2003), Vadose zone flow model uncertainty as conditioned on geophysical data, *Ground Water*, *41*(2), 119–127, doi:10.1111/j.1745-6584.2003.tb02576.x.

Callegary, J. B., T. P. A. Ferre, and R. W. Groom (2007), Vertical spatial sensitivity and exploration depth of low-induction-number electromagnetic-

induction instruments, *Vadose Zone J.*, *6*(1), 158–167, doi:10.2136/vzj2006.0120.

Chanasyk, D. S., and M. A. Naeth (1996), Field measurement of soil moisture using neutron probes, *Can. J. Soil Sci.*, *76*(3), 317–323, doi:10.4141/cjss96-038.

Day-Lewis, F. D., and J. W. Lane (2004), Assessing the resolution-dependent utility of tomograms for geostatistics, *Geophys. Res. Lett.*, *31*, L07503, doi:10.1029/2004GL019617.

Day-Lewis, F. D., K. Singha, and A. M. Binley (2005), Applying petrophysical models to radar travel time and electrical resistivity tomograms: Resolution-dependent limitations, *J. Geophys. Res.*, *110*, B08206, doi:10.1029/2004JB003569.

Desilets, D., M. Zreda, and T. P. A. Ferre (2010), Nature's neutron probe: Land surface hydrology at an elusive scale with cosmic rays, *Water Resour. Res.*, *46*, W11505, doi:10.1029/2009WR008726.

Evett, S. R., and J. L. Steiner (1995), Precision of neutron-scattering and capacitance type soil-water content gauges from field calibration, *Soil Sci. Soc. Am. J.*, *59*(4), 961–968, doi:10.2136/sssaj1995.03615995005900040001x.

Ferre, P. A., D. L. Rudolph, and R. G. Kachanoski (1996), Spatial averaging of water content by time domain reflectometry: Implications for twin rod probes with and without dielectric coatings, *Water Resour. Res.*, *32*(2), 271–279, doi:10.1029/95WR02576.

Franz, T. E., M. Zreda, P. A. Ferre, and C. Zweck (2011), Understanding the spatiotemporal distribution of soil moisture in a southern Arizonan dryland, Abstract H52A-03 presented at 2011 Fall Meeting, AGU, San Francisco, Calif., 5–9 Dec.

Furman, A., T. P. A. Ferre, and A. W. Warrick (2003), A sensitivity analysis of electrical resistivity tomography array types using analytical element modeling, *Vadose Zone J.*, *2*(3), 416–423.

Gardner, W., and D. Kirkham (1952), Determination of soil moisture by neutron scattering, *Soil Sci.*, *73*(5), 391–402, doi:10.1097/00010694-195205000-00007.

Glasstone, S., and M. C. Edlund (1952), *Elements of Nuclear Reactor Theory*, Van Nostrand, New York.

Grayson, R. B., A. W. Western, F. H. S. Chiew, and G. Bloschl (1997), Preferred states in spatial soil moisture patterns: Local and nonlocal controls, *Water Resour. Res.*, *33*(12), 2897–2908, doi:10.1029/97WR02174.

Greacen, E. L. (1981), *Soil Water Assessment by the Neutron Method*, Commonw. Sci. and Indust. Res. Org., Melbourne, Australia.

Hendrick, L. D., and R. D. Edge (1966), Cosmic-ray neutrons near Earth, *Phys. Rev.*, *145*(4), 1023, doi:10.1103/PhysRev.145.1023.

Hillel, D. (1998), *Environmental Soil Physics*, Academic, San Diego, Calif.

Hinnell, A. C., T. P. A. Ferré, J. A. Vrugt, J. A. Huisman, S. Moysey, J. Rings, and M. B. Kowalsky (2010), Improved extraction of hydrologic information from geophysical data through coupled hydrogeophysical inversion, *Water Resour. Res.*, *46*, W00D40, doi:10.1029/2008WR007060.

Hornbuckle, G., S. Irvin, and J. Patton (2011), Impact of Rapidly Growing Vegetation on COSMOS Measurements, Abstract 243-4 presented at 2011 ASA, CSSA, SSSA Annual Meeting, San Antonio, Tex., 16–19 Oct.

Jackson, T. J., P. E. Oneill, and C. T. Swift (1997), Passive microwave observation of diurnal surface soil moisture, *IEEE Trans. Geosci. Remote Sens.*, *35*(5), 1210–1222, doi:10.1109/36.628788.

Katul, G., A. Porporato, and R. Oren (2007), Stochastic dynamics of plant-water interactions, *Annu. Rev. Ecol. Evol. Syst.*, *38*, 767–791, doi:10.1146/Annurev.Ecolsys.38.091206.095748.

McNeill, J. D. (1980), Electromagnetic terrain conductivity measurement at low induction numbers, *Tech. Note TN-6*, edited, Geonics Limited of Mississagua, Ontario, Canada.

Milbrandt, A. (2005), A geographic perspective on the current biomass resource availability in the United States, *NREL/TP-560–39181*, National Renewable Energy Laboratory, Golden, Colorado.

Pelowitz, D. B. (Ed.) (2005), MCNPX user's manual, version 5, *Rep. LA-CP-05–0369*, Los Alamos Natl. Lab., Los Alamos, N. M.

Philip, J. R. (1969), Hydrostatics and hydrodynamics in swelling soils, *Water Resour. Res.*, *5*(5), 1070, doi:10.1029/WR005i005p01070.

Robinson, D. A., et al. (2008), Advancing process-based watershed hydrological research using near-surface geophysics: A vision for, and review of, electrical and magnetic geophysical methods, *Hydrol. Processes*, *22*(18), 3604–3635, doi:10.1002/hyp.6963.

Rosolem, R., M. Zreda, C. Zweck, T. E. Franz, W. J. Shuttleworth, X. Zeng, D. Desilets, P. A. Ferre, and S. Stillman (2011), Can a COSMOS probe measure other environmental variables other than water content in the soils?, Abstract H23H-1371 presented at 2011 Fall Meeting, AGU, San Francisco, Calif., 5–9 Dec.

Schaap, M. G., F. J. Leij, and M. T. van Genuchten (2001), ROSETTA: A computer program for estimating soil hydraulic parameters with hierarchical pedotransfer functions, *J. Hydrol.*, *251*(3–4), 163–176, doi:10.1016/S0022-1694(01)00466-8.

Simunek, J., M. T. van Genuchten, and M. Sejna (2008), Development and applications of the HYDRUS and STANMOD software packages and related codes, *Vadose Zone J.*, *7*(2), 587–600, doi:10.2136/Vzj2007.0077.

Topp, G. C., J. L. Davis, and A. P. Annan (1980), Electromagnetic determination of soil-water content - measurements in coaxial transmission-lines, *Water Resour. Res.*, *16*(3), 574–582, doi:10.1029/WR016i003p00574.

Zreda, M., D. Desilets, T. P. A. Ferre, and R. L. Scott (2008), Measuring soil moisture content non-invasively at intermediate spatial scale using cosmic-ray neutrons, *Geophys. Res. Lett.*, *35*, L21402, doi:10.1029/2008GL035655.

Zreda, M., W. J. Shuttleworth, X. Xeng, C. Zweck, D. Desilets, T. E. Franz, R. Rosolem, and P. A. Ferre (2012), COSMOS: The Cosmic-ray Soil Moisture Observing System, *Hydrol. Earth Syst. Sci. Discuss.*, *9*, 4505–4551, doi:10.5194/hessd-9-4505-2012.

Zweck, C., M. Zreda, and D. Desilets (2011), Empirical confirmation of the sub-kilometer footprint of cosmic-ray soil moisture probes, Abstract EGU2011-13393 presented at EGU General Assembly 2011, Vienna, Austria, 3–8 Apr.